

## Nonlocal labeling of paths in a single-photon interferometer

M. J. Pysher,\* E. J. Galvez, K. Misra, K. R. Wilson, B. C. Melius, and M. Malik

*Department of Physics and Astronomy, Colgate University, Hamilton, NY 13346*

(Received 24 August 2005; published 22 November 2005)

We prepared polarization-entangled photon pairs and sent one of the photons through a Mach-Zehnder interferometer. The apparatus was arranged so that when going through each arm of the interferometer the pairs were in a different Bell state. The distinguishability of the interferometer paths was determined by projecting the entangled state of the two photons with a polarizer placed in the path of the photon that does not go through the interferometer. As a consequence, actions on the remote photon determined nonlocally the visibility of the interference pattern. We present a full theoretical analysis and experimental results that confirm the theoretical predictions.

DOI: [10.1103/PhysRevA.72.052327](https://doi.org/10.1103/PhysRevA.72.052327)

PACS number(s): 03.67.Mn, 03.65.Ud, 42.50.Dv

Since the famous discussions of Einstein and Bohr at the 1927 Solvay conference, interference of quanta has been used to understand the most striking consequences of quantum superposition [1]. Feynman was particularly illuminating in his famous explanations, by putting quantum interference in terms of the distinguishability of the paths [2]. In the last two decades there have been numerous demonstrations of the interference of quanta as applied to understanding quantum mechanics. A particularly important one is the “quantum eraser,” whereby the distinguishability of the paths in an interferometer, manifested by changes in the visibility of the interference, was modified after the interferometer [3]. The possibility of choosing the determination of paths after the interferometer [4] was labeled “delayed choice” by Wheeler [1]. In such experiments, entanglement between the quanta and the apparatus leads to a selection of a subset of data that reveals or not the distinguishable information [5]. Superposition of two quanta in a nonseparable form, named “entanglement” by Schrödinger, has been used to demonstrate the striking nonlocality prediction of quantum mechanics that was highlighted by the Einstein, Podolski, and Rosen (EPR) *gedankenexperiment* [6]. This nonlocal correlation between entangled quanta has been exploited recently in fundamentally new ways, from quantum teleportation [7] to quantum communication and computation schemes [8,9].

The idea of a scheme that combines single-particle interference and polarization entanglement was considered recently [10,11]. The essence of the concept is to send a photon through an interferometer and specify the distinguishability of the paths by manipulating the entangled partner that does not go through the interferometer. In the work of Ref. [10], the slits of a double-slit interferometer had quarter-wave plates placed in front of them. The interference pattern produced by one polarization-entangled photon was made to appear or disappear by switching the orientation of a polarizer in the path of the entangled partner. The setting of the polarizer determined the labeling of the slits via the polarization of the light.

In this article we report experiments that used entangle-

ment to label the paths of a Mach-Zehnder interferometer. We did this by manipulating the entangled state of two photons such that in each arm of the interferometer the photon pair was in a different Bell state. The projection of the state of the pair of photons via a polarizer in the path of the remote photon determined the distinguishability of the interferometer paths. As a consequence, the visibility of the interference pattern could be continuously varied by action on an entangled partner in a remote location. In this article we explore all possible ways in which this nonlocal determination can be achieved with interference of Bell states in an interferometer. Since we performed this work, we became aware of a recent discussion of a similar idea [12], and of a recent experiment of this type [13].

Maximally entangled Bell states are expressed as [14]

$$|\Phi^\pm\rangle = \frac{1}{\sqrt{2}}(|H\rangle_1|H\rangle_2 \pm |V\rangle_1|V\rangle_2), \quad (1a)$$

$$|\Psi^\pm\rangle = \frac{1}{\sqrt{2}}(|H\rangle_1|V\rangle_2 \pm |V\rangle_1|H\rangle_2), \quad (1b)$$

where the polarization of the photons 1 and 2 are expressed in the basis  $(H, V)$  that represents the horizontal and vertical polarizations.

Let us consider the experiment represented schematically in Fig. 1. The source  $S$  produces pairs of polarization-entangled photons in the state  $|\Phi^+\rangle$ . Photon 1 goes toward a detector and photon 2 goes through a Mach-Zehnder interferometer and then to a detector. When arm A of the inter-

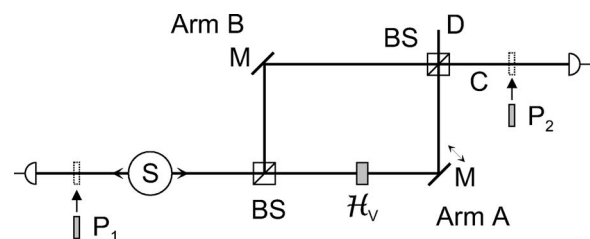


FIG. 1. Schematic of the experiment to measure the interference of the Bell states  $\Phi^+$  and  $\Phi^-$ .

\*Present address: Dept. of Physics, U. of Virginia.

ferometer is blocked, the entangled state with photon 2 going through arm *B* is  $|\Phi^+\rangle$ . Arm *A* of the interferometer has a half-wave plate  $\mathcal{H}_V$  aligned with the vertical axis (*V*) that inserts a phase  $\pi$  between the states  $|H\rangle$  and  $|V\rangle$ . Thus when arm *B* is blocked, the entangled state of the photon pair with photon 2 going through arm *A* is  $|\Phi^-\rangle$ .

Upon passing the interferometer with its two arms open the state of the photon pair is split into two parts defined by the output ports of the second beam splitter,

$$|\psi\rangle = (tr|\Phi^+\rangle + rt|\Phi^-\rangle e^{i\delta})|c\rangle + (rr|\Phi^+\rangle + tt|\Phi^-\rangle e^{i\delta})|d\rangle, \quad (2)$$

where  $r$  and  $t$  are the reflection and transmission coefficients of the beam splitters in the interferometer and  $\delta$  is the phase difference due to the path-length difference between the two arms. Let  $|c\rangle$  and  $|d\rangle$  represent the spatial mode of the wave functions of the light going in the directions of ports *C* and *D*, respectively. The probability amplitudes for going in directions *C* and *D* contain the interference of the two Bell states  $|\Phi^+\rangle$  and  $|\Phi^-\rangle$ . We will refer to the interference of these two Bell states as case I. As shown in Fig. 1, we only detect photon 2 leaving the output port *C* of the interferometer.

Similarly to Eqs. (1a) and (1b), we now define the states  $|\Phi'^{\pm}\rangle$  and  $|\Psi'^{\pm}\rangle$  in terms of the basis ( $H', V'$ ) that is rotated by an angle  $\theta_1$  relative to the ( $H, V$ ) basis. It can be shown that the following relations between the Bell states in the two bases hold:

$$|\Phi^+\rangle = |\Phi'^+\rangle, \quad (3a)$$

$$|\Phi^-\rangle = \cos 2\theta_1 |\Phi'^-\rangle - \sin 2\theta_1 |\Psi'^+\rangle, \quad (3b)$$

$$|\Psi^+\rangle = \cos 2\theta_1 |\Psi'^+\rangle + \sin 2\theta_1 |\Phi'^-\rangle, \quad (3c)$$

$$|\Psi^-\rangle = |\Psi'^-\rangle. \quad (3d)$$

The relations given above specify the polarization correlations that are commonly used for demonstrations of nonlocality and violations of Bell's inequalities [15].

We now place a polarizer  $P_1$  in the path of photon 1. If the transmission axis of  $P_1$  forms an angle  $\theta_1$  relative to the horizontal, then we can associate the state of the transmitted photon with  $|H'\rangle$ . In general, the states of Eq. (3) would get respectively projected by  $P_1$  onto the states

$$|\Phi_p^+\rangle = |H'\rangle_1 |H'\rangle_2, \quad (4a)$$

$$|\Phi_p^-\rangle = |H'\rangle_1 (\cos 2\theta_1 |H'\rangle_2 - \sin 2\theta_1 |V'\rangle_2), \quad (4b)$$

$$|\Psi_p^+\rangle = |H'\rangle_1 (\sin 2\theta_1 |H'\rangle_2 + \cos 2\theta_1 |V'\rangle_2), \quad (4c)$$

$$|\Psi_p^-\rangle = |H'\rangle_1 |V'\rangle_2. \quad (4d)$$

Following Eq. (2), the probability of detecting the pair after this projection is

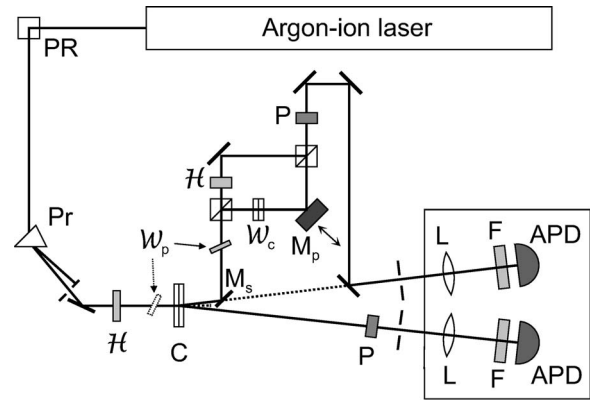


FIG. 2. Diagram of the experimental apparatus. The optical components shown are: steering/elevator mirrors ( $PR$ ), prism ( $Pr$ ), half-wave plates ( $\mathcal{H}$ ), state-tuning wave plate ( $\mathcal{W}_p$ ), BBO crystals ( $C$ ), mirrors ( $M_s$  and  $M_p$ ), compensating wave plates ( $\mathcal{W}_c$ ), polarizers ( $P$ ), lenses ( $L$ ), filters ( $F$ ) and avalanche photodiode detectors (APD).

$$P^I = |rt\langle H' \rangle_1 [\langle H' \rangle_2 + (\cos 2\theta_1 |H'\rangle_2 - \sin 2\theta_1 |V'\rangle_2) e^{i\delta}]|^2, \quad (5a)$$

$$= \frac{1}{2} (1 + \cos 2\theta_1 \cos \delta), \quad (5b)$$

where we have applied the condition that the beam splitters have  $r^*r = t^*t = 1/2$ . The detection probability will show oscillations (i.e., fringes) as a function of  $\delta$  with a visibility given by  $V = \cos 2\theta_1$ . When  $\theta_1 = 0$  one can understand the interference as arising due to the indistinguishability of paths *A* and *B*, because it leaves both photons in the state  $|H'\rangle$ , irrespective of the interferometer path. Conversely, when  $\theta_1 = \pi/4$  there is no interference because the paths become distinguishable by the polarization of photon 2, with  $|H'\rangle_2$  specifying arm *B* (polarization oriented  $+\pi/4$  to the horizontal axis), and  $|V'\rangle_2$  specifying arm *A* (polarization oriented  $-\pi/4$  to the horizontal axis). The interesting aspect of this experiment is that the degree of distinguishability of the photon going through the interferometer (i.e., the visibility) is determined by the orientation of the polarizer in the path of the photon *not* going through the interferometer.

We performed experiments to verify these predictions. The laboratory arrangement is shown in Fig. 2. A 457.9-nm beam from an argon-ion laser was incident on a pair of crossed beta-barium-borate crystals to produce polarization-entangled photon pairs via type-I spontaneous parametric down conversion [16]. The two crystals, 1 mm in thickness, were cut at a phase matching angle of  $26.2^\circ$ , which produced a 3-degree cone of down-converted photons at the degenerate wavelength of 915.8 nm. As shown in Fig. 2, down-converted photons labeled “1” went to a detector arrangement consisting of an iris, a focusing lens, a 10-nm bandpass filter, and an avalanche photodiode. Photons labeled “2” went through a Mach-Zehnder interferometer before going to a detection arrangement similar to the one for photon 1. Glan-Thompson polarizers  $P_1$  and  $P_2$  were placed in the path of photons 1 and 2 to project their correlated state.

The interferometer was composed of two nonpolarizing 50-50 cube beam splitters and two dielectric mirrors. To interfere the entangled states of case I the interferometer had a 2-mm thick first-order quartz half-wave plate in arm *A* with its fast axis oriented vertically ( $\mathcal{H}_v$ ). Arm *B* of the interferometer had two 1-mm thick quartz wave plates ( $\mathcal{W}_c$ ) with their fast axes aligned horizontally and vertically, respectively. They compensated the optical path length of the half-wave plate without introducing any phases between the polarization eigenstates. The use of compensating optics of the same material as the wave plates simplified the alignment of the interferometer.

The birefringence of the down-conversion crystal [16], and nonideal reflection phases given to the light by the steering mirror  $M_s$ , introduced a phase  $\alpha$  between the polarization states. As a consequence, the state of the photon pairs before photon 2 entered the interferometer was

$$|\psi\rangle = \frac{1}{\sqrt{2}}(|H\rangle_1|H\rangle_2 + e^{i\alpha}|V\rangle_1|V\rangle_2). \quad (6)$$

We set  $\alpha$  to the desired value by tilting a wave plate  $\mathcal{W}_p$  [16], which introduces a compensating phase between the vertical and horizontal components. For some of the experiments reported here  $\mathcal{W}_p$  was a zero-order wave plate placed before the interferometer, as shown in Fig. 2. In other experiments  $\mathcal{W}_p$  was a multiple-order wave plate located before the down-conversion crystals. To get state  $|\Phi^+\rangle$  when photon 2 was going through arm *B* of the interferometer (i.e., adjusting  $\alpha=0$ ), we blocked arm *A*, placed a polarizer  $P_2$  after the interferometer, and tilted  $\mathcal{W}_p$  until the measurement of the polarization correlations satisfied Eq. (4a). Our analysis of this correlation accounted for the mirror inversion produced by  $M_s$ . We verified the entanglement further by performing a Clauser-Horne-Shimony-Holt test of Bell's inequalities, which gave  $S=2.21\pm 0.07$  (local behavior is restricted to  $S < 2$  [17]). After  $\mathcal{W}_p$  was adjusted, we blocked arm *B* of the interferometer and verified the correlations of Eq. (4b).

One of the dielectric mirrors of the interferometer ( $M_p$  in Fig. 2) was mounted on two translation stages. One stage was used to adjust the length of the arms of the interferometer to be equal, via the observation of white-light fringes. A piezoelectric stack was placed as a spacer in the other stage. By scanning the voltage applied to the piezostack  $v_p$  we were able to slightly change the length of one of the arms, and thus vary the phase difference  $\delta$  over several optical periods. The pulse output of the photodetectors was fed to data acquisition electronics that recorded the singles and the coincidences. Each data run recorded counts acquired during 15 s for each setting of  $v_p$ , which was stepwise increased.

Figure 3 shows the coincidence counts (in 15 s) as a function of the phase difference  $\delta/2\pi$  obtained for values of  $\theta_1$  from 0 to  $\pi/4$  taken in increments of  $\pi/12$ . They confirm the predictions presented above. The data were fitted by the function  $N_0[1+V \cos \delta(v_p)]$ , with fitting parameters  $N_0$ ,  $V$ , and the phase  $\delta(v_p)$ , which had a cubic dependence on  $v_p$  due to the nonlinearity of the piezoelectric.

The fits show the visibility starting at  $V=0.73\pm 0.07$  for  $\theta_1=0$  (circles), and evolving through  $V=0.68\pm 0.06$  for  $\theta_1$

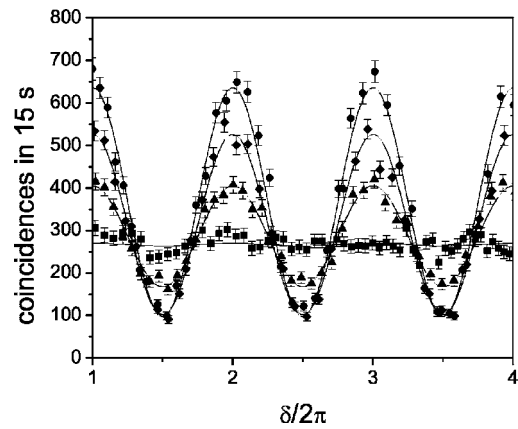


FIG. 3. Data for Case I for  $\theta_1=0$  (circles),  $\theta_1=\pi/12$  (diamonds),  $\theta_1=\pi/6$  (triangles), and  $\theta_1=\pi/4$  (squares).

for  $\theta_1=\pi/12$  (diamonds),  $V=0.42\pm 0.07$  for  $\theta_1=\pi/6$  (triangles), and reaching  $V=0.01\pm 0.09$  for  $\theta_1=\pi/4$  (squares). After performing several tests, we concluded that the variation in the constant term  $N_0(\theta_1)$  for the different data sets [ $N_0(0)=367\pm 20$ ,  $N_0(\pi/12)=314\pm 17$ ,  $N_0(\pi/6)=286\pm 17$ ,  $N_0(\pi/4)=267\pm 16$ ] was due to misalignments of the small-aperture Glan-Thompson polarizer  $P_1$  as it was rotated.

We also present the results of what we label as case II. By setting the half-wave plate in arm *A* of the interferometer to form an angle of  $\pi/4$  with the horizontal ( $\mathcal{H}_{\pi/4}$ ) we rotated the polarization of the light going through that arm by  $\pi/2$  (i.e., exchanging  $|V\rangle$  and  $|H\rangle$  in the state of the photon going through arm *A*). In this new arrangement, shown in Fig. 4, we put the pair of photons in state  $|\Psi^+\rangle$  when arm *B* is blocked and photon 2 is going through arm *A*. The detection probability then becomes

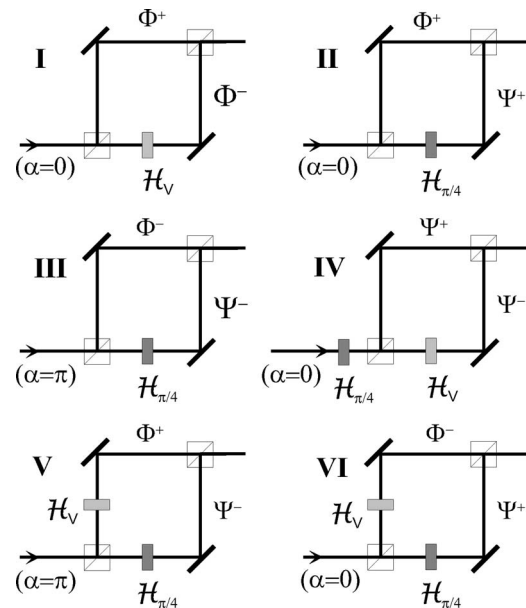


FIG. 4. Schemes for interfering Bell states in an interferometer. The source produces entangled photons in the state given by Eq. (6). Other components are half-wave plates  $\mathcal{H}_v$  with its fast axis vertical and  $\mathcal{H}_{\pi/4}$  with its fast axis at  $\pi/4$  with the horizontal.

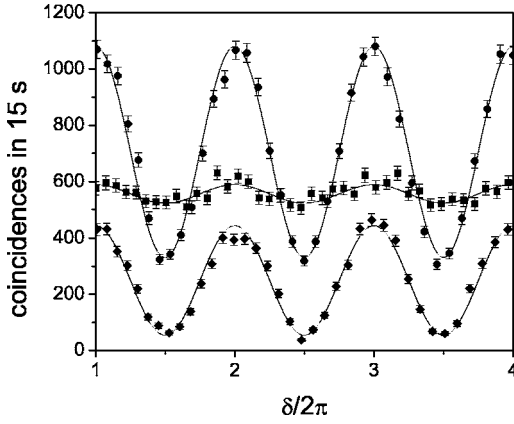


FIG. 5. Data for case II for  $\theta_1 = \pi/4$  (circles) and  $\theta_1 = 0$  (squares) without polarizer  $P_2$ , and for  $\theta_1 = 0$  when  $P_2$  is present with  $\theta_2 = \pi/4$  (diamonds).

$$P^{\text{II}} = |rt\langle H' \rangle_1 [ |H' \rangle_2 + (\sin 2\theta_1 |H' \rangle_2 + \cos 2\theta_1 |V' \rangle_2 ) e^{i\delta} ]|^2, \quad (7a)$$

$$= \frac{1}{2} (1 + \sin 2\theta_1 \cos \delta). \quad (7b)$$

Equation (7a) is similar to Eq. (5a) but controlled by polarizer  $P_1$  in a different way: the interferometer paths become indistinguishable when  $\theta_1 = \pi/4$  and distinguishable when  $\theta_1 = 0$ . In the latter case, arms A and B of the interferometer are associated with states  $|H' \rangle_2$  (vertical polarization) and  $|V' \rangle_2$  (horizontal polarization), respectively. Our measurements for  $\theta_1 = \pi/4$  and  $\theta_1 = 0$  are shown by the circles and the squares in Fig. 5, respectively ( $N_0 = 705 \pm 26$  and  $V = 0.53 \pm 0.05$ , and  $N_0 = 556 \pm 24$  and  $V = 0.06 \pm 0.06$ , respectively). They indeed confirm the predictions.

The nonzero visibility of the data for  $\theta_1 = 0$  is a reasonable outcome given that the resolution of the rotating mounts holding the optical elements is about  $1^\circ$ . The same may be true for the case of  $\theta_1 = \pi/4$ , where an error in the orientation angle of the half-wave plate in arm A may result in a small admixture of  $|\Phi^+\rangle$  with  $|\Psi^+\rangle$  for light going through arm A, affecting the visibility of the interference.

Returning to case I, when  $\theta_1 = \pi/4$  the projected state of the entangled pair [Eq. (5a)] reveals the path information via the polarization state of photon 2. We now place a polarizer  $P_2$  in the path of photon 2 after the interferometer. If the transmission axis of  $P_2$  forms an angle  $\theta_2$  with respect to the horizontal axis, then the state of the pair of photons gets projected to a single product state  $|H' \rangle_1 |H'' \rangle_2$ . The final state thus has no path information, and the probability takes a simpler form,

$$P_{\text{ER}}^{\text{I}} = |rt\langle H' \rangle_1 |H'' \rangle_2 [ \cos(\theta_2 - \pi/4) + \sin(\theta_2 - \pi/4) e^{i\delta} ]|^2, \quad (8a)$$

$$= \frac{1}{4} [1 + \sin 2(\theta_2 - \pi/4) \cos \delta]. \quad (8b)$$

When  $\theta_2 = \pi/2$  in Eq. (8b) we regain the case of indistinguishable paths with full visibility. In such a case polarizer

$P_2$  is said to have “erased” locally the path information [5]. We obtained the same situation in case II by setting  $\theta_1 = 0$  to make the paths distinguishable, and by setting  $\theta_2 = \pi/4$  to locally erase the path information with full fringe visibility [i.e., giving a probability identical to Eq. (8b)]. The data for the local path erasure in case II is shown by the diamonds in Fig. 5 (fitted parameters were  $N_0 = 249 \pm 15$  and  $V = 0.78 \pm 0.07$ ).

Superpositions of  $|\Psi^-\rangle$  with either  $|\Phi^-\rangle$  or  $|\Psi^+\rangle$  (cases III and IV, respectively) lead to similar cases of interference visibility controlled by  $\theta_1$ . The setup to interfere these states is shown in Fig. 4. In case III, which we verified, wave plate  $\mathcal{W}_P$  is adjusted so that  $\alpha = \pi$ . In case IV the half-wave plate  $\mathcal{H}_{\pi/4}$  is put before the interferometer and  $\mathcal{W}_P$  is adjusted so that  $\alpha = \pi$ .

The superpositions between  $|\Phi^+\rangle$  and  $|\Psi^-\rangle$  (case V), and between  $|\Phi^-\rangle$  and  $|\Psi^+\rangle$  (case VI) lead to independence of  $\theta_1$ . For example, for case V the paths are distinguishable and thus yields no interference. The probability is given by

$$P^{\text{V}} = |rt\langle H' \rangle_1 ( |H' \rangle_2 + |V' \rangle_2 e^{i\delta} )|^2 = \frac{1}{2}. \quad (9)$$

The preparation of these last two cases is shown in Fig. 4. Notice that it involves the same components but with different values of  $\alpha$ . It is interesting to consider the local erasure probability for these two cases when  $P_2$  is present. The probability can be shown to be given by

$$P_{\text{ER}}^{\text{V}} = \frac{1}{4} [1 + \sin 2(\theta_2 - \theta_1) \cos \delta], \quad (10a)$$

$$P_{\text{ER}}^{\text{VI}} = \frac{1}{4} [1 + \sin 2(\theta_2 + \theta_1) \cos \delta]. \quad (10b)$$

While there is an absence of fringes when  $P_2$  is not present, we see that when  $P_2$  is placed after the interferometer the visibility of the locally erased distinguishability is dependent on  $\theta_1$ . Thus, if we include the polarizer behind the interferometer, the visibility of the interference can be varied remotely after all.

We have verified the predictions of Eqs. (9) and (10) for cases V and VI by taking scans of coincidences vs path length for different settings of  $P_1$  without  $P_2$  and with  $P_2$  in different settings, similar to the scans of Fig. 5. The verification of case VI presented the most challenge to us. The settings of the wave plates in the interferometer (see Fig. 4) combined with the 10-nm bandwidth of the filters in front of the detectors made the output very sensitive to the dispersion of the zero-order wave plates. As a result we were not able to measure the expected zero visibility for any orientation of  $P_1$  with  $P_2$  absent. We corrected this by narrowing the bandwidth of the down-converted light. This was done by placing a 1-nm filter in front of one of the detectors. To underscore the correlations between the down-converted photons we did the verifications with the 1-nm filter placed in front of the remote detector [18].

The above interferometric correlations are not limited to pure Bell states. We have verified a case that produces effects similar to those of cases V and VI, where there is indepen-

dence of the visibility with  $\theta_1$  when  $P_2$  is absent. The states of the light when going through arms  $A$  and  $B$  of the interferometer were  $2^{-1/2}(|H\rangle_1|H\rangle_2 + i|V\rangle_1|V\rangle_2)$  and  $2^{-1/2}(|H\rangle_1|V\rangle_2 + i|V\rangle_1|H\rangle_2)$ , respectively. When  $P_2$  is placed the detection probability is a more complex function of the angles, or  $(1 + \sin 2\theta_2 \cos \delta - \sin 2\theta_1 \cos 2\theta_2 \sin \delta)/4$ .

In cases where the polarization correlation is flipped in only one of the arms, such as in cases II and IV, the results cannot be reproduced, even qualitatively, by incoherent mixtures of product states (mixed states) [13]. In the other cases, the control of visibilities by actions on the remote photon may be reproduced qualitatively but not quantitatively. This is because the control of the visibilities is not due to nonlocal labeling of paths, but rather by superposition of out-of-phase interference patterns.

In summary, we have shown that polarization-entangled photons can be used to interfere Bell states in an interferometer. The visibility of the fringes that are produced when the path length of the interferometer is varied was determined by projecting the state of the photons using polarizers. By projecting the state either remotely by action of a polarizer on the photon that does not go through the interferometer, or locally by action of a polarizer after the interferometer, we

can select many ways in which we can determine the distinguishability of the paths and consequently vary the visibility of the interference pattern. In essence, this is a more general form of the quantum eraser [10,13] than previously considered (see, for example, Ref. [5]). Since the which-way information is obtained by manipulations on the remote photon, this experiment can easily be turned into one of state manipulation by delayed choice, where the path information can be chosen to be absent, recovered, or erased by projections of the state of two correlated photons, done by delayed actions on the photon that does not go through the interferometer. Because the labeling of the paths is done by entangling the quantum system with the apparatus, the which-way labeling is not an irreversible disturbance of the system [19]. Interferometry using these schemes may lead to new ideas for quantum computation with linear optical elements and manifestations of nonlocality.

We thank M. Beck, S. Hinterlong, P. Kwiat, S. Malin, V. Mansfield, D. Simeonov and R. Williams for help and useful discussions. This work was funded by National Science Foundation Grant Nos. DUE-9952626 and PHY-9988004.

- 
- [1] J. A. Wheeler and W. H. Zurek, *Quantum Theory and Measurement* (Princeton University Press, Princeton, NJ, 1983).
- [2] R. P. Feynman, R. B. Leighton, and M. Sands, *The Feynman Lectures on Physics* (Addison-Wesley, Reading, PA, 1965), Vol. 3, p. 1-1.
- [3] M. O. Scully and K. Drühl, *Phys. Rev. A* **25**, 2208 (1982).
- [4] Y.-H. Kim, R. Yu, S. P. Kulik, Y. Shih, and M. O. Scully, *Phys. Rev. Lett.* **84**, 1 (2000).
- [5] P. D. D. Schwindt, P. G. Kwiat, and B.-G. Englert, *Phys. Rev. A* **60**, 4285 (1999).
- [6] A. Einstein, B. Podolsky, and N. Rosen, *Phys. Rev.* **47**, 777 (1935).
- [7] D. Bouwmeester, J.-W. Pan, K. Mattle, M. Eibl, H. Weinfurter, and A. Zeilinger, *Nature* **390**, 575 (1997).
- [8] W. Tittel and G. Weihs, *Quantum Inf. Comput.* **1**, 3 (2001).
- [9] *The Physics of Quantum Information*, edited by D. Bouwmeester, A. Ekert, and A. Zeilinger (Springer, Berlin, 2000).
- [10] S. P. Walborn, M. O. Terra Cunha, S. Padua, and C. H. Monken, *Phys. Rev. A* **65**, 033818 (2002).
- [11] A. Zeilinger, *Rev. Mod. Phys.* **71**, S288 (1999).
- [12] P. G. Kwiat and B.-G. Englert, in *Science and Ultimate Reality*, edited by J. D. Barrow *et al.* (Cambridge University Press, Cambridge, England, 2004).
- [13] A. Gogo, W. D. Snyder, and M. Beck, *Phys. Rev. A* **71**, 052103 (2005).
- [14] K. Mattle, H. Weinfurter, P. G. Kwiat, and A. Zeilinger, *Phys. Rev. Lett.* **76**, 4656 (1996).
- [15] P. G. Kwiat, K. Mattle, H. Weinfurter, A. Zeilinger, A. V. Sergienko, and Y. Shih, *Phys. Rev. Lett.* **75**, 4337 (1995).
- [16] P. G. Kwiat, E. Waks, A. G. White, I. Appelbaum, and P. H. Eberhard, *Phys. Rev. A* **60**, R773 (1999).
- [17] J. F. Clauser, M. A. Horne, A. Shimony, and R. A. Holt, *Phys. Rev. Lett.* **23**, 80 (1969).
- [18] E. J. Galvez, C. H. Holbrow, M. J. Pysher, J. W. Martin, N. Courtemanche, L. Heilig, and J. Spencer, *Am. J. Phys.* **73**, 127 (2005).
- [19] T. J. Herzog, P. G. Kwiat, H. Weinfurter, and A. Zeilinger, *Phys. Rev. Lett.* **75**, 3034 (1995).